Review TRENDS in Biotechnology Vol.23 No.3 March 2005

Physicochemical perspectives on DNA microarray and biosensor technologies

Rastislav Levicky[1] and Adrian Horgan[2]

[1]Department of Chemical Engineering, Columbia University, 500 West 120th Street, New York, NY, USA
[2]Solexa Ltd, Chesterford Research Park, Little Chesterford, Nr Saffron Walden, Essex, CB101XLT, UK

Detection and sequence-identification of nucleic acid molecules is often performed by binding, or hybridization, of specimen 'target' strands to immobilized, complementary 'probe' strands. A familiar example is provided by DNA microarrays used to carry out thousands of solid-phase hybridization reactions simultaneously to determine gene expression patterns or to identify genotypes. The underlying molecular process, namely sequence-specific recognition between complementary probe and target molecules, is fairly well understood in bulk solution. However, this knowledge proves insufficient to adequately understand solid-phase hybridization. For example, equilibrium binding constants for solid-phase hybridization can differ by many orders of magnitude relative to solution values. Kinetics of probe–target binding are affected. Surface interactions, electrostatics and polymer phenomena manifest themselves in ways not experienced by hybridizing strands in bulk solution. The emerging fundamental understanding provides important insights into application of DNA microarray and biosensor technologies.

Introduction

Solid-phase hybridization, in which nucleic acid strands tethered to a solid support bind DNA or RNA molecules from solution, underpins the modern microarray and biosensor biotechnologies now widely used for genotyping, studying gene expression and for biological detection [1–6]. Applications of these tools have increased tremendously as is evident, for example, in the number of scientific publications in this area (Figure 1). Microarrays, in which thousands of hybridization reactions are carried out in parallel, are commonly used for addressing fundamental questions in biology and for sample characterization up to whole-genome scale. Biosensors tend to be dedicated to specific tasks, such as detection of a small number of analyte sequences, with data acquisition often performed in real-time.

In solid-phase or 'surface' hybridization, association of immobilized strands, referred to as 'probes', with 'target' sequences from solution occurs at a solid–liquid interface. The interfacial environment is distinct from the bulk solution; thus, surface hybridization might be anticipated to deviate from expectations solely based on knowledge of solution hybridization. These differences are crucial to guiding device design, formulating assay protocols and developing data analysis tools. Because of space constraints, discussion of surface modification chemistries, detection methods and alternate hybridization schemes (such as those employing hydrogel matrices [7,8]) has been omitted. Much of this additional information is available in other recent reviews [9–11].

Corresponding author: Levicky, R. (rl268@columbia.edu).
Available online 26 January 2005

Background

As with all natural processes, solid-phase hybridization is subject to thermodynamic and kinetic constraints [12]. Thermodynamics define limits on discrimination of different target sequences and detection of low copy targets. Kinetics determine how quickly equilibrium is approached. Kinetic considerations also include mass transport, which is well understood within standard transport theory. The following discussion therefore focuses on the hybridization reaction itself.

Kinetics

In the simplest model, hybridization is treated as a one-step reversible reaction with rate constants k_f and k_r (P: probe; T: target; D: duplex):

$$P + T \underset{k_r}{\overset{k_f}{\rightleftarrows}} D \qquad \text{(Equation 1)}$$

The forward reaction is assumed to proceed at a rate $k_f\,(1-f)\,P_0.C_T$, whereas the reverse rate is $k_r\,.\,f.P_0$. P_0 is the total surface density (number of strands/unit of area) of probes of which a fraction f is hybridized; thus $(1-f)\,P_0$ is the surface density of unhybridized probes. C_T is the bulk concentration of target molecules. Equilibrium is characterized by the equality of forward and reverse rates:

$$k_f.C_T(1-f)P_0 = k_r.f.P_0 \text{ OR } f/(C_T(1-f)) = k_f/k_r = K_E \qquad \text{(Equation 2)}$$

where K_E is the equilibrium constant. At the outset of hybridization $f=0$, the forward rate is maximum and the reverse rate is zero. As hybridization proceeds f increases and C_T decreases; these changes result in a decrease of the forward rate k_f and an increase in the reverse rate. Within this basic picture, Figure 2 plots the forward and reverse rates as a function of time for two values of k_r assuming $k_f C_T$ is fixed. The case characterized by smaller k_r approaches equilibrium more slowly. Because k_r varies strongly with sequence, such considerations directly impact on achievement of equilibrium in microarray

 0167-7799/$ - see front matter doi:10.1016/j.tibtech.2005.01.004

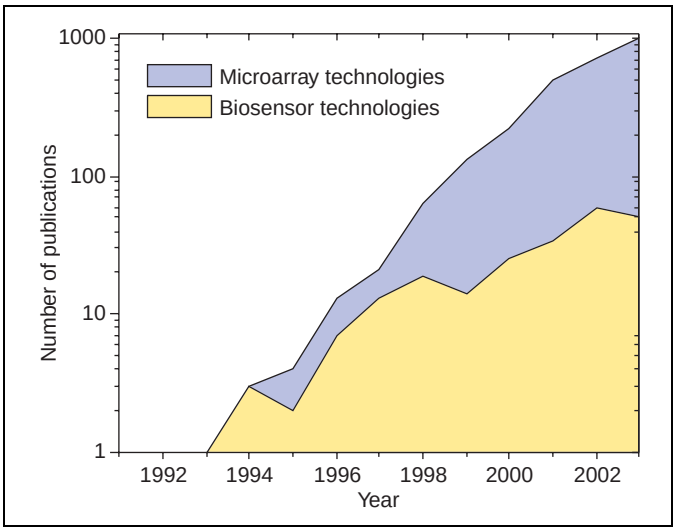

Figure 1. Annual trend in number of publications for DNA microarrays and biosensors (Data used with permission from Web of Science®).

assays in which numerous probe–target sequences hybridize simultaneously [13]. The simplicity of this one-step model is convenient but belies the true complexity of hybridization. A more detailed model, consistent with empirical data on solution hybridization, is based on an initial formation of a double-stranded, marginally-stable 'nucleus' of a few base pairs; after this relatively slow nucleation the rest of the surrounding sequence zips-up rapidly [14,15].

Thermodynamics

Translating understanding of solution hybridization to the surface case is central to designing probe sets for microarrays and for interpreting experimental data [16–20]. Hybridization thermodynamics in bulk solution are sufficiently well understood to allow prediction of standard free energies (ΔG°) and equilibrium association constants $K_E = \exp(-\Delta G^\circ/RT)$ (R: gas constant; T: absolute temperature) from nearest-neighbor models [21]. Figure 3 illustrates the thermodynamic relationship between solution and solid-phase hybridization. In solution hybridization (Figure 3a), probe strands P and target strands T combine to form duplex D with a free energy change ΔG_2°. By contrast, in solid-phase hybridization (Figure 3b) a strand T must penetrate into a layer of P strands to hybridize, with an overall free energy change ΔG_{Tot}°. Applying the thermodynamic tenet that free energy changes depend only on initial and final states, surface hybridization can be broken down into three hypothetical steps as in Figure 3c: (i) release of a P strand into solution; (ii) hybridization with a T strand under solution conditions; and (iii) immobilization of the duplex D formed. The associated change in free energy is $\Delta G_{Tot}^\circ = \Delta G_1^\circ + \Delta G_2^\circ + \Delta G_3^\circ$ and the equilibrium binding or association constant for solid-phase hybridization K_{ES} is:

$$K_{ES} = K_{EB}\exp(-(\Delta G_1^\circ + \Delta G_3^\circ)/RT) \qquad \text{(Equation 3)}$$

$$K_{EB} = \exp(-\Delta G_2^\circ/RT)$$

where K_{EB} is the bulk solution equilibrium constant. The factor $\exp[-(\Delta G_1^\circ + \Delta G_3^\circ)/RT]$ 'corrects' K_{EB} so that the product describes the situation of solid-phase hybridization. If $\Delta G_1^\circ = -\Delta G_3^\circ$ then bulk and surface hybridization would be thermodynamically equivalent. In general, this equivalence will not be obeyed because the extraction of a single-stranded P (step 1) is not simply a reversal of an insertion of a double-stranded D (step 3) because single- and double-stranded molecules are expected to interact differently with the probe film environment owing to differences in size, charge, rigidity or other molecular properties.

Interpretation of experimental data on solid-phase hybridization can pose significant challenges. For example, although end-attachment of probes is often the intended scenario, it can be difficult to confirm and some ostensibly end-immobilization chemistries might lead to cross-linking at internal sites, resulting in multipoint attachment that can hinder association with target molecules. Caution is also warranted with regard to achievement of hybridization equilibrium. Equilibrium can be convincingly demonstrated if the same final state is reached from different initial states; such controls, however, are usually not available. This article is based on studies representing well-defined situations; nonetheless, the original reports remain the best source for ascertaining the experimental conditions of a particular study.

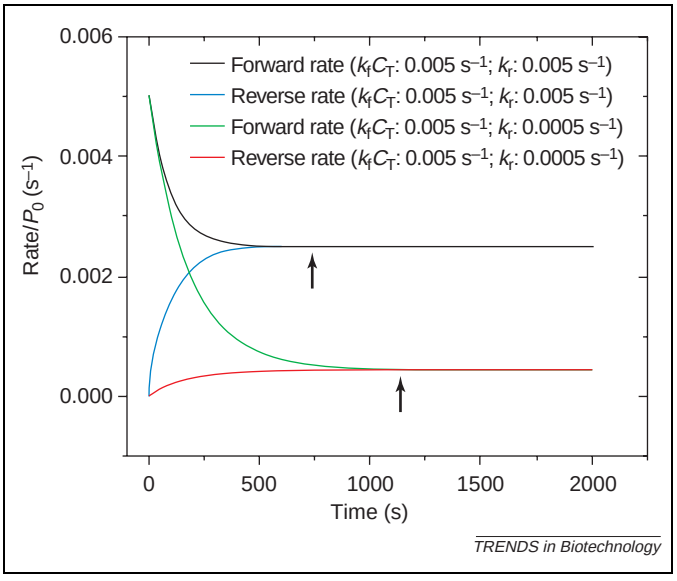

Figure 2. Approach to equilibrium (approximated by arrows) for two combinations of forward (k_f) and reverse (k_r) rates, based on the simple hybridization model of the form *probe + target ↔ duplex*. P_0 on the *y*-axis is the total surface coverage of probes; see Equation 2.

Comparison of solid-phase (K_{ES}) and bulk (K_{EB}) equilibrium constants

Figure 4 compares experimental values of K_{ES} with K_{EB} values calculated for the same sequences and conditions as outlined in [21]. The K_{ES} data represent four different studies employing end-tethered probe strands 10–30 nucleotides long hybridizing to fully complementary, same-length targets [22–25]. Four different immobilization chemistries, ionic strengths from 0.1–1 M, and temperatures from 10–70 °C were used. K_{ES} was derived either from measurements of the hybridized fraction f [22,23,25] or from the ratio of forward and reverse rate constants [24] (see Equation 2). Measurements were carried out *in situ*

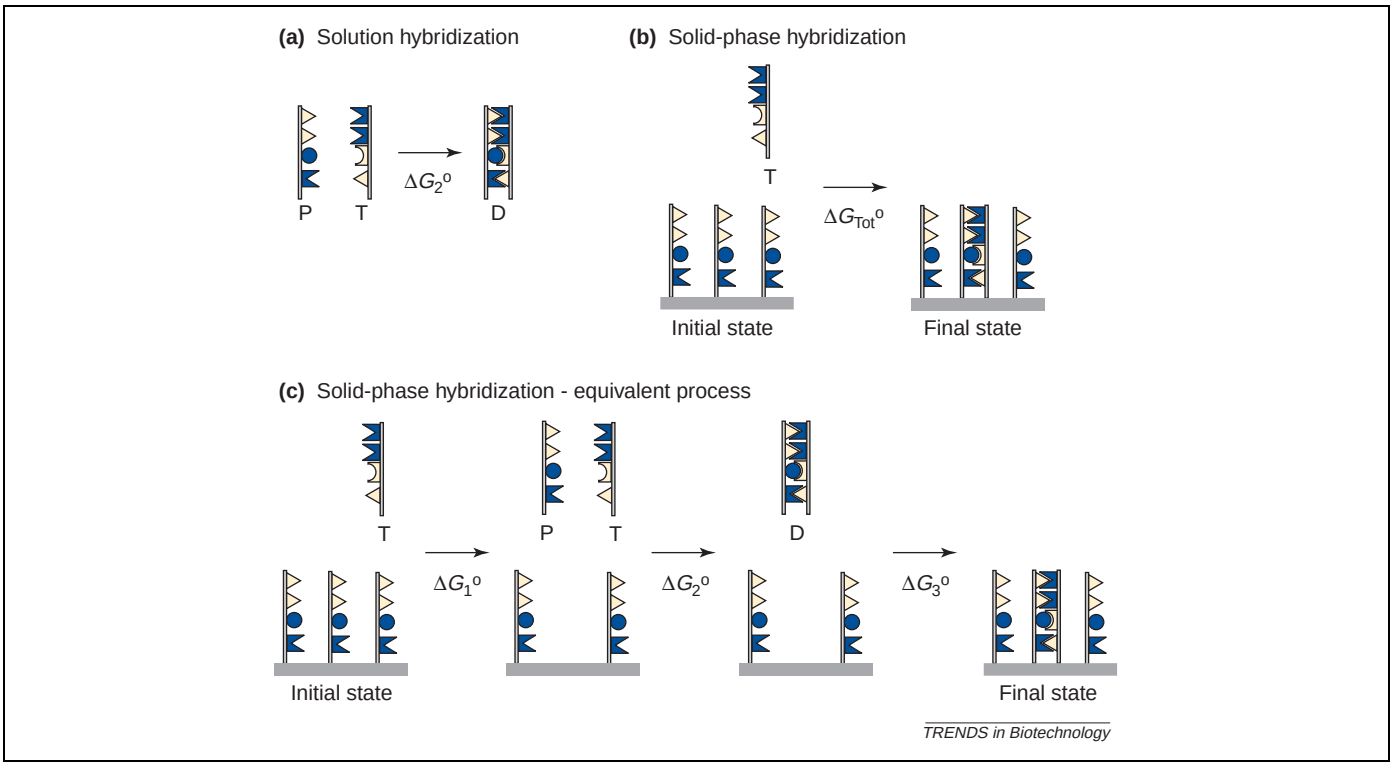

Figure 3. Schematic depiction of solution **(a)** and solid-phase **(b)** hybridization, and definition of the associated free energy changes. In **(c)**, solid-phase hybridization is decomposed into three steps, the second of which is thermodynamically equivalent to solution hybridization. Abbreviations: P, probe strand; T, target strand; D, duplex strand.

so that perturbation owing to washing of hybridized surfaces was avoided. It is noteworthy that, in this spectrum of conditions, K_{ES} falls in a narrow range of $\sim$5 decades whereas K_{EB} varies over $>$30 decades. This indicates that bulk solution and surface thermodynamics are not equivalent; that is, $\Delta G_1^\circ \neq -\Delta G_3^\circ$. Usually K_{ES} is suppressed relative to K_{EB} (right of dashed line in Figure 4), although data also indicate that hybridization on a surface can be more thermodynamically favored than in solution (left of dashed line). Suppression of K_{ES} relative to K_{EB} might reflect electrostatic and steric penalties associated with penetration of a target strand into a probe layer. On the other hand, a high local concentration of probes might stabilize binding of targets in states not possible under solution conditions, leading to $K_{ES} > K_{EB}$ [25]. Analysis of data obtained from commercial microarrays suggests that solid-phase hybridization is less thermodynamically favored than hybridization of the same sequences in solution [20].

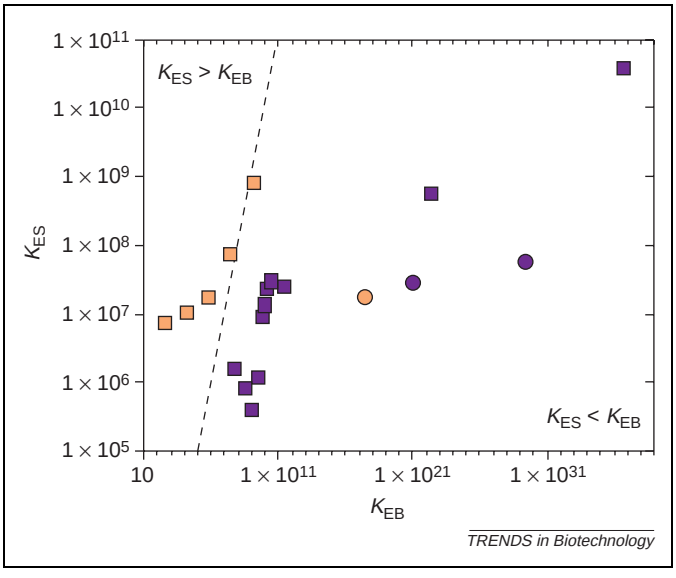

Figure 4. Comparison of equilibrium constants for solid-phase (K_{ES}) and bulk solution (K_{EB}) hybridization. K_{ES} values were taken from references [22] (orange circle), [23] (purple circles), [24] (purple squares) and [25] (orange squares), collectively spanning ionic strengths 0.1–1 M, temperatures 10–70 °C, and strand lengths 10–30 nucleotides. K_{EB} was calculated according to reference [21]. The data show that variation in K_{ES} over these conditions is much more modest ($\sim$5 decades) than for K_{EB} ($\sim$30 decades). The dashed line represents $K_{ES} = K_{EB}$.

That thermodynamics of solution and surface hybridization differ is perhaps not surprising. Typically, oligonucleotide probe films are characterized by a coverage of between 10^{12} to 10^{13} probes/cm^2 and a layer thickness of several nanometers [26]. These values translate to a local concentration of $\sim$0.1–1 M in nucleotides, much higher than when hybridization is carried out in solution, implying a very different local environment for solid-phase hybridization.

Impact of probe layer structure

Experiments indicate that surface hybridization is suppressed when the coverage of probe molecules is too high [27–32]. For end-tethered 25mer (i.e. 25 nucleotides long) probes Steel *et al.* reported close to 100% hybridization to complementary targets under 1 M ionic strength when probe coverage was below $\sim 4 \times 10^{12}$ cm^{-2}, with a sharp fall off in hybridization extents at higher coverages [27]. An alternate measure of probe–target affinity is melting temperature T_M, defined as that temperature at which

half of hybridizable probes remain single-stranded while in equilibrium with target solution of fixed composition [33–35]. A T_M decrease of nearly 10 °C, corresponding to decreased stability of hybridized probe–target pairs, was reported when the density of 20mer probes increased from $\sim 1\times?10^{11}$ cm^{-2} to $\sim 4\times10^{12}$ cm^{-2} [34,35]. Thus changes in both T_M and hybridization extents indicate that solid-phase hybridization is disfavored at high probe coverages.

Because nucleic acids carry a minus one charge per nucleotide, electrostatic effects might be expected to be partially responsible for destabilization of probe–target binding. A theory developed by Vainrub and Pettitt [36] derives an electrostatic correction factor corresponding to $\exp[-(\Delta G_1^\circ+\Delta G_3^\circ)/RT]$ (compare with Equation 3). This theory models the probe layer as a plane with a smeared charge density $\sigma(f)$ (charge/area) where f denotes extent of hybridization as before. Suppression of T_M is also predicted. A subsequent analysis of the impact of competitive hybridization on solid-phase assays by Halperin *et al.* treats the probe film as three-dimensional with a smeared and uniform charge density $\rho(f)=\sigma(f)/H$, where H is the film thickness [37]. Both analyses find that the electrostatic part of $\Delta G_1^\circ+\Delta G_3^\circ$ increases linearly with probe coverage (i.e. density of immobilized charge); however, a different dependence on concentration of bulk salt is predicted.

Probe coverage also affects hybridization kinetics, as evident from a decrease in initial rates of hybridization at higher probe densities [28,38]. Henry *et al.* reported that k_f for hybridization of end-tethered 22mers in 0.11 M ionic strength was five times slower than in solution when probe coverage was 1.4×10^{12} cm^{-2}, and ten times slower when probe coverage increased to 2.8×10^{12} cm^{-2} [38]. Peterson *et al.* also observed a slowdown in hybridization with increasing probe coverage [28]. Hagan and Chakraborty developed a theory describing kinetics of solid-phase hybridization. These authors adapted methods from polymer science [39,40] to model solid-phase hybridization subject to configurational statistics of polymer chains [41]. The forward hybridization rate was predicted to decrease with probe coverage P_0 as $k_f\sim P_0^{-1.8}$ in reasonable agreement with experimental trends [41]. Understanding how polymer phenomena impact solid-phase hybridization is not yet complete. One study investigating assembly of probe films suggested that polymer configurational effects became important once probe length exceeded 20 nucleotides [42].

In the limits of sparse films, when probes are too far apart to come into contact, patches of bare surface will be accessible to adsorption of target strands. In this limit targets might first adsorb and then diffuse along the solid support before hybridizing to a probe [43]. The additional pathway provided by such 'two-dimensional' (2D) hybridization is predicted to enhance hybridization rates [43,44]. Comparison of theoretical expectations to experimental data showed evidence of 2D enhancement for hybridization of 20mers at coverages of $\sim 7\times10^{10}$ cm^{-2} [44,45]. The impact of 2D enhancement would be expected to diminish when complex target mixtures are assayed because much of the accessible surface around a probe will become occupied by other (non-complementary) target sequences, and also if surface treatments to suppress nonspecific adsorption are employed.

The influence of strand length was investigated for end-tethered 10mer, 20mer, and 30mer probe–target pairs at a fixed probe coverage of 1.2×10^{13} cm^{-2} [24]. The forward hybridization rate k_f increased with strand length, as might be expected if longer probe-target pairs present more sites for initiation of duplex formation. Intriguingly, experimental dependence of k_f on length L was significantly stronger ($k_f\sim L^{2.5}$) than suggested by theoretical arguments ($k_f\sim L^{0.7}$) [41]. Using polymeric (116–2057 nt) probes and targets, Stillman and Tonkinson also observed increased hybridization rates with probe size [46]. Graves and coworkers investigated hybridization of polymeric (157–864 nt) targets to oligonucleotide probes [47]. A delay in onset of hybridization was observed, increasing from 1 h to 8 h with target length at a fixed target concentration of 4×10^{-8} M. By contrast, a 20mer target hybridized in less than 5 min. The delay was postulated to reflect initial formation of relatively weakly surface-adsorbed target states, which only slowly rearranged into stable probe–target duplexes capable of withstanding the washing protocol.

The structure of a probe layer is asymmetric in that it is bounded by a solid support from one side. This asymmetry suggests that the location of a particular base along a probe strand might influence its impact on hybridization. Using surface plasmon resonance, Georgiadis and coworkers monitored hybridization between a 25mer probe and two 18mer targets that hybridized at different locations on the probe [23]. Solution thermodynamics of both target–probe pairs were equivalent. Target 18low hybridized to the first 18 bases at the tethered end of the probe, whereas 18hi hybridized to the last 18 bases at the free end. At a sparse coverage of 1.5×10^{12} cm^{-2}, both targets hybridized at the same rate. By contrast, when probe coverage increased to 3×10^{12} cm^{-2}, 18hi hybridized about three times faster. These results suggest presence of an activation barrier associated with target penetration into the probe film, which is also expected on theoretical grounds [41]. In their study of 60mer oligonucleotide arrays, Hughes *et al.* [48] found that base mismatches further away from the surface exerted a stronger effect on hybridization. These results similarly suggest that probe accessibility to hybridization improves with increased distance from the surface, consistent with earlier studies in which incorporation of molecular spacers to displace probes from the solid support led to higher hybridization yields [49,50].

Proximity to a solid support also implies that surface interactions will be present. This issue is somewhat intractable in that it is specific to the modification chemistry employed. Using single-molecule spectroscopy, Osborne *et al.* observed multiple fluorescence behaviors from isolated DNA probes immobilized through an amine endgroup to 3′-glycidoxypropyltrimethoxysilane modified silica [51]. The fluorescence data suggest that the labeled probes can exist in different arrangements on the surface. Just ~5% of the probes were active toward targets, indicating that surface chemistry was prominent in governing hybridization activity. Suppressed hybridization in the presence of strong probe–surface interactions has been also reported by others [26]. In some instances surface

interactions can be tuned to achieve a specific effect. On conductive supports application of electric fields can enhance mismatch discrimination [52], alter orientation of immobilized DNA molecules [53] and accelerate hybridization kinetics [47]. Vainrub and Pettitt have recently extended their theoretical model [36] to discuss the role of surface electrostatics [54].

When present, intramolecular structure, whether in probe or target species, can strongly influence hybridization yields. Using a tRNA target, Mir and Southern observed high hybridization yields when the new duplex region was optimally accommodated within the native tRNA structure, for example, through stacking with native double-stranded regions. [55]

Effect of temperature and ionic strength

Higher temperatures are often reported to increase the forward rate of solid-phase hybridization [38,45,56]. On the other hand, using 10mer probes at a coverage of 1.2×10^{13} cm^{-2}, Okahata *et al.* observed that k_f did not strongly depend on temperature although k_r increased significantly so that equilibrium was still reached ~60 times faster at 30 °C than at 15 °C [24] (see Figure 2). Increase in ionic strength from 0.1 to 0.5 M NaCl increased k_f about six-fold while decreasing k_r by an order of magnitude [24]. These trends qualitatively agree with solution behavior. [57] In solution, higher ionic strength stabilizes double-stranded structure leading to faster k_f and slower k_r. Higher temperature causes k_r to increase whereas k_f can increase, stay the same or even decrease. The varied response of k_f is attributed to temperature dependence of forming a hybridization nucleus [57].

Impact of mismatches on solid-phase hybridization

A crucial consideration for applications is the ability to discriminate mismatched from fully complementary targets. Using 25mer end-tethered probes and 25mer targets, Peterson *et al.* found that mismatches at one or two base positions slowed down approach to equilibrium at probe coverages of 3×10^{12} cm^{-2}, accompanied by features in hybridization vs time curves suggestive of multiple structural rearrangements [23]. By contrast, at a more sparse probe coverage of 1.5×10^{12} cm^{-2} the rate of hybridization was similar for matched and mismatched targets. This suggests that probe density is a key factor governing the influence of mismatches. Forman *et al.* observed that a central mismatch in a 20mer probe–target pair did not influence hybridization kinetics [58]. Okahata *et al.* studied hybridization of 20mers at a probe coverage of 1.2×10^{13} cm^{-2}, finding that k_f decreased and k_r increased for mismatched sequences [24]. The overall effect was that approach to equilibrium was faster for mismatched than for complementary targets. The impact of mismatches on hybridization between 60mer probes and synthetic mRNA polymers was investigated by Dai *et al.* [13]. In contrast to the other studies, samples containing a complex mixture of target sequences were used. Under these conditions, mismatched targets achieved equilibrium faster than fully complementary ones. Usage of kinetic data to better identify signals arising from mismatched targets was suggested [13].

The diversity of experimental observations regarding influence of mismatches could in part reflect formation of structures more complex than one-to-one hybridization. For example, a target molecule can bridge and hybridize across multiple probes (Figure 5b). Compared with a complementary target, the presence of a mismatch might facilitate bridging by destabilizing duplex formation at the location of the bridge (Figure 5c). The progression through bridging or other structures during the approach to equilibrium would be expected to depend on details of sequence, including mismatches, on the probe spacing, and on probe and target lengths.

Bhanot *et al.* developed a computer model of hybridization in a microarray type experiment, accounting for a complex sample background. [19] It was shown that cross-hybridization, involving binding of mismatched probe–target pairs in competition with perfect complements, can profoundly slow down approach to equilibrium. Poor specificity of the probe set, and thus increased susceptibility to cross-hybridization, translated to increased 'concentration bias' in which true concentration of rarer targets was underestimated and that of more abundant ones was overestimated. This is an important consideration for gene expression studies if levels of gene activity are to be estimated from concentrations of mRNA targets.

Modeling of data from microarrays

Application of physical models to microarray data has been undertaken in several recent studies [18,20,59]. The relationship of solution target concentration C_T to the extent of hybridization f, as monitored by fluorescence intensity I, was shown to exhibit nonlinear behavior owing to saturation of probe sites with targets at high C_T. The nonlinear response agreed with a Langmuir isotherm form [20,59]. Held *et al.* showed that I increased with more favorable free energy of hybridization ΔG_2° between fully complementary probe-target pairs, with the consequence that strongly binding sequences exhibited chemical saturation at lower C_T. [20] This is an important consideration for selection of microarray probe sequences [18]. Moreover, background signal from mismatched targets scaled exponentially with ΔG_2°, indicating that high affinity

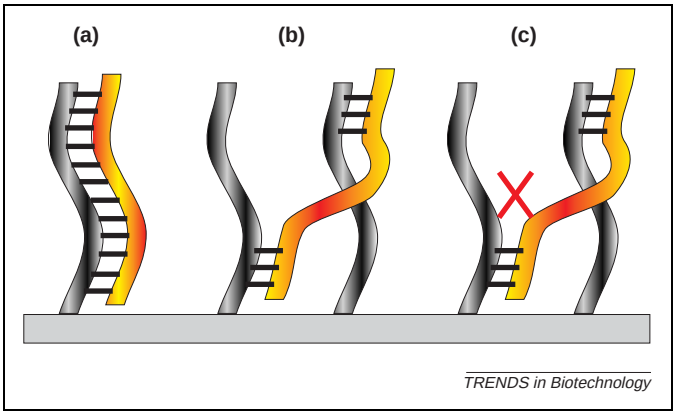

Figure 5. **(a)** One-to-one hybridization. **(b)** A target bridge across two probe strands. **(c)** A target bridge facilitated by a mismatch (cross).

probes are also more susceptible to association with targets that are only partially complementary [18,20]. The impact of dye label incorporation into target strands on thermodynamics of probe-target association has also been theoretically modeled. [60] Significantly, most microarray experiments involve a washing step to improve stringency of sequence discrimination; the perturbation this represents to hybridization equilibria is an important question yet to be addressed.

Conclusions

Solid-phase hybridization, as practiced in DNA biosensor and microarray technologies, is a more complex process than solution hybridization. Although recent years brought significant progress in physical understanding of solid-phase hybridization, many aspects crucial both to applications and to fundamental insight, remain unresolved. Among these, perhaps the foremost questions include identifying the origin of the difference between K_{ES} and K_{EB} (see Figure 4), establishing how solution conditions and probe layer structure affect discrimination of mismatches and understanding key factors influencing hybridization kinetics. Resolution of these issues will require close interaction between experimentalists and theorists, and between researchers who aim to understand solid-phase hybridization under precisely defined conditions (e.g. equilibrium, characterized surfaces and target solutions) on one hand and technology practitioners faced with complex sample mixtures and experimental protocols on the other.

References

1 Mir, K.U. and Southern, E.M. (2000) Sequence variation in genes and genomic DNA: Methods for large-scale analysis. *Annu. Rev. Genomics Hum. Genet.* 1, 329–360
2 Schena, M. *et al*. (1998) Microarrays: Biotechnology's discovery platform for functional genomics. *Trends Biotechnol.* 16, 301–306
3 Graves, D.J. (1999) Powerful tools for genetic analysis come of age. *Trends Biotechnol.* 17, 127–134
4 Wang, J. (2002) Electrochemical nucleic acid biosensors. *Anal. Chim. Acta* 469, 63–71
5 D'Orazio, P. (2003) Biosensors in clinical chemistry. *Clin. Chim. Acta* 334, 41–69
6 Vercoutere, W. and Akeson, M. (2002) Biosensors for DNA sequence detection. *Curr. Opin. Chem. Biol.* 6, 816–822
7 Kolchinsky, A. and Mirzabekov, A. (2002) Analysis of SNPs and other genomic variations using gel-based chips. *Hum. Mutat.* 19, 343–360
8 Jensen, K.K. *et al*. (1997) Kinetics for hybridization of peptide nucleic acids (PNA) with DNA and RNA studied with the BIAcore technique. *Biochemistry* 36, 5072–5077
9 Beaucage, S.L. (2001) Strategies in the preparation of DNA oligonucleotide arrays for diagnostic applications. *Curr. Med. Chem.* 8, 1213–1244
10 Pirrung, M.C. (2002) How to make a DNA chip. *Angew. Chem.-Int. Edit.* 41, 1276–1289
11 Tarlov, M.J. and Steel, A.B. (2003) DNA-Based Sensors (Chapter 12). In *Biomolecular Films: Design, Function, and Applications* (Rusling, J.F., ed.), pp. 545–608, Marcel Dekker
12 Wetmur, J.G. (1991) DNA probes: Applications of the principles of nucleic acid hybridization. *Crit. Rev. Biochem. Mol. Biol.* 26, 227–259
13 Dai, H. *et al*. (2002) Use of hybridization kinetics for differentiating specific from non-specific binding to oligonucleotide microarrays. *Nucleic Acids Res.* 30, e86 (http://nar.oupjournals.org/cgi/content/abstract/30/16/e86)
14 Wetmur, J.G. and Davidson, N. (1968) Kinetics of renaturation of DNA. *J. Mol. Biol.* 31, 349–370
15 Porschke, D. and Eigen, M. (1971) Co-operative non-enzymic base recognition 3. Kinetics of helix-coil transition of the oligoribouridylic: oligoriboadenylic acid system and of oligoriboadenylic acid alone at acidic pH. *J. Mol. Biol.* 62, 361–381
16 Li, F. and Stormo, G.D. (2001) Selection of optimal DNA oligos for gene expression arrays. *Bioinformatics* 17, 1067–1076
17 Rouillard, J-M. *et al*. (2002) OligoArray: Genome-scale oligonucleotide design for microarrays. *Bioinformatics* 18, 486–487
18 Mei, R. *et al*. (2003) Probe selection for high-density oligonucleotide arrays. *Proc. Natl. Acad. Sci. U. S. A.* 100, 11237–11242
19 Bhanot, G. *et al*. (2003) The importance of thermodynamic equilibrium for high throughput gene expression arrays. *Biophys. J.* 84, 124–135
20 Held, G.A. *et al*. (2003) Modeling of DNA microarray data by using physical properties of hybridization. *Proc. Natl. Acad. Sci. U. S. A.* 100, 7575–7580
21 SantaLucia, J. (1998) A unified view of polymer, dumbbell, and oligonucleotide DNA nearest-neighbor thermodynamics. *Proc. Natl. Acad. Sci. U. S. A.* 95, 1460–1465
22 Nelson, B.P. *et al*. (2001) Surface plasmon resonance imaging measurements of DNA and RNA hybridization adsorption onto DNA microarrays. *Anal. Chem.* 73, 1–7
23 Peterson, A.W. *et al*. (2002) Hybridization of mismatched or partially matched DNA at surfaces. *J. Am. Chem. Soc.* 124, 14601–14607
24 Okahata, Y. *et al*. (1998) Kinetic measurements of DNA hybridisation on an oligonucleotide-immobilized 27-MHz quartz crystal microbalance. *Anal. Chem.* 70, 1288–1296
25 Stevens, P.W. *et al*. (1999) DNA hybridization on microparticles: Determining capture-probe density and equilibrium dissociation constants. *Nucleic Acids Res.* 27, 1719–1727
26 Levicky, R. *et al*. (1998) Using self-assembly to control the structure of DNA monolayers on gold: A neutron reflectivity study. *J. Am. Chem. Soc.* 120, 9787–9792
27 Steel, A.B. *et al*. (1998) Electrochemical quantitation of DNA immobilized on gold. *Anal. Chem.* 70, 4670–4677
28 Peterson, A.W. *et al*. (2001) The effect of surface probe density on DNA hybridization. *Nucleic Acids Res.* 29, 5163–5168
29 Jin, L. *et al*. (2003) Preparation of end-tethered DNA monolayers on siliceous surfaces using heterobifunctional cross-linkers. *Langmuir* 19, 6968–6975
30 Podyminogin, M.A. *et al*. (2001) Attachment of benzaldehyde-modified oligodeoxynucleotide probes to semicarbazide-coated glass. *Nucleic Acids Res.* 29, 5090–5098
31 Pena, S.R.N. *et al*. (2002) Hybridization and enzymatic extension of Au nanoparticle-bound oligonucleotides. *J. Am. Chem. Soc.* 124, 7314–7323
32 Walsh, M.K. *et al*. (2001) Optimizing the immobilization of single-stranded DNA onto glass beads. *J. Biochem. Biophys. Methods* 47, 221–231
33 Peterlinz, K.A. *et al*. (1997) Observation of hybridization and dehybridization of thiol- tethered DNA using two-color surface plasmon resonance spectroscopy. *J. Am. Chem. Soc.* 119, 3401–3402
34 Watterson, J.H. *et al*. (2000) Effects of oligonucleotide immobilization density on selectivity of quantitative transduction of hybridization of immobilized DNA. *Langmuir* 16, 4984–4992
35 Watterson, J.H. *et al*. (2002) Towards the optimization of an optical DNA sensor: control of selectivity coefficients and relative surface affinities. *Anal. Chim. Acta* 457, 29–38
36 Vainrub, A. and Pettitt, B.M. (2002) Coulomb blockage of hybridization in two-dimensional DNA arrays. *Phys. Rev. E Stat. Nonlin. Soft Matter Phys.* 66, 041905
37 Halperin, A. *et al*. (2004) Sensitivity, specificity, and the hybridization isotherms of DNA chips. *Biophys. J.* 86, 718–730
38 Henry, M.R. *et al*. (1999) Real-time measurements of DNA hybridization on microparticles with fluorescence resonance energy transfer. *Anal. Biochem.* 276, 204–214
39 Misra, S. *et al*. (1989) A polyelectrolyte brush theory. *Macromolecules* 22, 4173–4179
40 Milner, S. (1992) Competitive adsorption kinetics of end-adsorbing polymers. *Macromolecules* 25, 5487–5494
41 Hagan, M.F. and Chakraborty, A.K. (2004) Hybridization dynamics of surface immobilized DNA. *J. Chem. Phys.* 120, 4958–4968
42 Steel, A.B. *et al*. (2000) Immobilization of nucleic acids at solid surfaces: Effect of oligonucleotide length on layer assembly. *Biophys. J.* 79, 975–981

43 Chan, V. *et al*. (1995) The biophysics of DNA hybridization with immobilized oligonucleotide probes. *Biophys. J.* 69, 2243–2255
44 Erickson, D. *et al*. (2003) Modeling of DNA hybridization kinetics for spatially resolved biochips. *Anal. Biochem.* 317, 186–200
45 Zeng, J. *et al*. (2003) Interfacial hybridization kinetics of oligonucleotides immobilized onto fused silica surfaces. *Sens. Actuators B* 90, 68–75
46 Stillman, B.A. and Tonkinson, J.L. (2001) Expression microarray hybridization kinetics depend on length of the immobilized DNA but are independent of immobilization substrate. *Anal. Biochem.* 295, 149–157
47 Su, H-J. *et al*. (2002) Kinetics of heterogeneous hybridization on indium tin oxide surfaces with and without an applied potential. *Electrophoresis* 23, 1551–1557
48 Hughes, T.R. *et al*. (2001) Expression profiling using microarrays fabricated by an ink-jet oligonucleotide synthesizer. *Nat. Biotechnol.* 19, 342–347
49 Guo, Z. *et al*. (1994) Direct fluorescence analysis of genetic polymorphisms by hybridization with oligonucleotide arrays on glass supports. *Nucleic Acids Res.* 22, 5456–5465
50 Shchepinov, M.S. *et al*. (1997) Steric factors influencing hybridisation of nucleic acids to oligonucleotide arrays. *Nucleic Acids Res.* 25, 1155–1161
51 Osborne, M.A. *et al*. (2001) Probing DNA surface attachment and local environment using single molecule spectroscopy. *J. Phys. Chem. B* 105, 3120–3126
52 Heaton, R.J. *et al*. (2001) Electrostatic surface plasmon resonance: Direct electric field- induced hybridization and denaturation in monolayer nucleic acid films and label-free discrimination of base mismatches. *Proc. Natl. Acad. Sci. U. S. A.* 98, 3701–3704
53 Kelley, S.O. *et al*. (1998) Orienting DNA helices on gold using applied electric fields. *Langmuir* 14, 6781–6784
54 Vainrub, A. and Pettitt, B.M. (2003) Surface electrostatic effects in oligonucleotide microarrays: Control and optimization of binding thermodynamics. *Biopolymers* 68, 265–270
55 Mir, K.U. and Southern, E.M. (1999) Determining the influence of structure on hybridization using oligonucleotide arrays. *Nat. Biotechnol.* 17, 788–792
56 Riccelli, P.V. *et al*. (2001) Hybridization of single-stranded DNA targets to immobilized complementary DNA probes: Comparison of hairpin versus linear capture probes. *Nucleic Acids Res.* 29, 996–1004
57 Bloomfield, V.A. *et al*. (2000) *Nucleic Acids - Structures, Properties, and Functions*, University Science Books, Sausalito, CA
58 Forman, J.E. *et al*. (1998) Thermodynamics of duplex formation and mismatch discrimination on photolithographically synthesized oligonucleotide arrays. *ACS Symp. Ser.* 682, 206–228
59 Hekstra, D. *et al*. (2003) Absolute mRNA concentrations from sequence-specific calibration of oligonucleotide arrays. *Nucleic Acids Res.* 31, 1962–1968
60 Naef, F. and Magnasco, M.O. (2003) Solving the riddle of the bright mismatches: Labeling and effective binding in oligonucleotide arrays. *Phys. Rev. E Stat. Nonlin. Soft Matter Phys.* 68, 011906